

This work was written as part of one of the author's official duties as an Employee of the United States Government and is therefore a work of the United States Government. In accordance with 17 U.S.C. 105, no copyright protection is available for such works under U.S. Law.

Public Domain Mark 1.0

<https://creativecommons.org/publicdomain/mark/1.0/>

Access to this work was provided by the University of Maryland, Baltimore County (UMBC) ScholarWorks@UMBC digital repository on the Maryland Shared Open Access (MD-SOAR) platform.

Please provide feedback

Please support the ScholarWorks@UMBC repository by emailing scholarworks-group@umbc.edu and telling us what having access to this work means to you and why it's important to you. Thank you.



Ephemeral Stream Network Extraction from Lidar-Derived Elevation and Topographic Attributes in Urban and Forested Landscapes

Marina J. Metes , Daniel K. Jones , Matthew E. Baker , Andrew J. Miller , Dianna M. Hogan , J.V. Loperfido, and Kristina G. Hopkins

Research Impact Statement: We describe a new approach using lidar-derived elevation data to remotely map headwater streams in forested and urban landscapes, and address ongoing challenges with mapping small streams.

ABSTRACT: Under-representations of headwater channels in digital stream networks can result in uncertainty in the magnitude of headwater habitat loss, stream burial, and watershed function. Increased availability of high-resolution (<2 m) elevation data makes the delineation of headwater channels more attainable. In this study, elevation data derived from light detection and ranging was used to predict ephemeral stream networks across a forested and urban watershed in the Maryland Piedmont USA. A method was developed using topographic openness (TO) and wetness index to remotely predict the extent of stream networks. Predicted networks were compared against a comprehensive field survey of the ephemeral network in each watershed to evaluate performance. Comparisons were also made to the U.S. Geological Survey National Hydrography Dataset (NHD) and a flow accumulation approach where a single drainage area threshold defined channel initiation. Although the NHD and flow accumulation methods resulted in low commission errors, omission errors were highest in these networks. The TO-based networks detected a larger number of ephemeral channels, but with higher commission error. Small ephemeral channels with less defined banks or originating at groundwater seeps were difficult to detect in all methods. Comparisons between forested and urban watersheds also highlight the difficulty of identifying headwater channels using topographic attributes in human-modified landscapes.

(**KEYWORDS:** headwater streams; channel heads; geomorphology; stream mapping; ephemeral; perennial; lidar; drainage network; topography.)

INTRODUCTION

Remotely mapping the existence of intermittent and ephemeral (non-perennial) streams is an ongoing challenge despite improvements in the resolution and spatial-temporal coverage of remote sensing data (Shanafield et al. 2021). The point of channel

initiation often represents a transition from dispersion dominated hillslope flow to convergent channel flow paths (Montgomery and Dietrich 1988; Montgomery and Foufoula-Georgiou 1993; Istanbuluoglu et al. 2002), but can also be controlled by a wide variety of physical forms depending on topographic setting, underlying geology, climate, and land use (Band 1993). During wet periods, the point of channel

Paper No. JAWR-20-0163-P of the *Journal of the American Water Resources Association* (JAWR). Received November 2, 2020; accepted May 11, 2022. © 2022 American Water Resources Association. This article has been contributed to by U.S. Government employees and their work is in the public domain in the USA. **Discussions are open until six months from issue publication.**

U.S. Geological Survey (Metes), Maryland-Delaware-District of Columbia Water Science Center Baltimore, Maryland, USA; U.S. Geological Survey (Jones), Utah Water Science Center West Valley City, Utah, USA; Department of Geography and Environmental Systems (Baker, Miller), University of Maryland, Baltimore County Baltimore, Maryland, USA; U.S. Geological Survey, Southeast Region (Hogan), Reston, Virginia, USA; Durham, North Carolina, USA; and U.S. Geological Survey (Hopkins), South Atlantic Water Science Center Raleigh, North Carolina, USA (Correspondence to Metes: mmetes@usgs.gov).

Citation: Metes, M.J., D.K. Jones, M.E. Baker, A.J. Miller, D.M. Hogan, J.V. Loperfido, and K.G. Hopkins. 0000. "Ephemeral Stream Network Extraction from Lidar-Derived Elevation and Topographic Attributes in Urban and Forested Landscapes." *JAWRA Journal of the American Water Resources Association* n/a–n/a. <https://doi.org/10.1111/1752-1688.13012>.

initiation can extend upslope along convergent contours, highlighting the variable extent of drainage networks in response to climate (Blyth and Rodda 1973). This variability in channel initiation further complicates our ability to remotely detect small streams with dynamic flow regimes (Shanfield et al. 2021).

An accurate representation of channel head locations is fundamental for linking hillslope and channel processes, ultimately controlling overall watershed dissection and network structure (Tribe 1990; Montgomery and Dietrich 1992; Walker and Willgoose 1999; Heine et al. 2004; Baker et al. 2007). Headwaters often represent more than 75% of total watershed channel length and are closely linked to nutrient dynamics, macroinvertebrate habitat, and groundwater-surface water exchanges (Gomi et al. 2002; Lindsay 2006; James et al. 2007; Elmore and Kaushal 2008; Downing et al. 2012; Messenger et al. 2021). Many studies have shown the functional importance of small, non-perennial headwater streams (Meyer and Wallace 2001; Meyer et al. 2007; Roy et al. 2009), so an accurate accounting of their presence on the landscape is key for effective management. Similarly, streamflow permanence is used to classify streams that are federally regulated under the Clean Water Act (The Navigable Waters Protection Rule 2020).

Watershed managers have historically used drainage networks comprised primarily of perennial streams when designing watershed management plans, such as the 'blue lines' from United States Geological Survey (USGS) topographic maps (Hansen 2001; Colson et al. 2008; Vance-Borland et al. 2009; Brooks and Colburn 2011; Elmore et al. 2013). The USGS National Hydrography Dataset (NHD), the digital equivalent of 'blue lines', is a nationally available dataset at the 1:100,000 scale that is widely used for watershed management and modeling applications (Hill et al. 2016; Thornbrugh et al. 2018; Wiczorek et al. 2018; Stewart et al. 2019). The NHD plus high resolution (NHDPlus HR; USGS 2018) at the scale of 1:24,000 or better is now being incorporated into national scale models with the increasing availability of data (Viger et al. 2016).

Field-based observations are commonly considered the most accurate means to identify channels but are seldom performed due to extensive time and labor requirements (McNamara et al. 2006). Therefore, efforts to remotely identify channels and extract drainage networks were initially developed from coarse (10 m or coarser resolution) digital topographic datasets (O'Callaghan and Mark 1984; Jenson and Domingue 1988; Tarboton et al. 1991; Band 1993; Heine et al. 2004). Many of these established methods for channel head and network extraction use topographic characteristics of upslope contributing drainage areas

to identify channel initiation points. Montgomery and Dietrich (1988) first suggested that a threshold between local topographic slope and contributing drainage area governs channel head locations. But, finer than 30-m resolution topographic data are necessary to identify channel heads on moderately steep and vegetated landscapes (Zhang and Montgomery 1994; Colson et al. 2006). A more common network delineation approach based on a single contributing drainage area threshold is frequently used despite documented inaccuracies (Heine et al. 2004; Lindsay 2006; James and Hunt 2010). These approaches fall under a category of techniques that attempt to emulate physical channel initiation processes from aggregate contributing drainage area variables and are thus referred to as channel initiation techniques (Lindsay 2006).

Other studies have explored topographic curvature and other morphologic indicators of valley shapes for network extraction (Tribe 1990, 1992; Tarboton and Ames 2001; Lindsay 2006; Sofia et al. 2011), hereafter referred to as valley recognition techniques. Channel initiation techniques are more widely used than valley recognition techniques due in part to a lack of topographic resolutions capable of representing fine-scale valley forms (Lindsay 2006). However, elevation data derived from light detection and ranging (lidar) and other high-resolution (<10 m) topographic datasets can resolve fine-scale topographic features essential for valley recognition techniques, and there have been considerable advances in extracting drainage networks from high-resolution topography. These techniques generally follow the same procedure of filtering a digital elevation model (DEM) to reduce noise, calculating and thresholding topographic attributes to extract a skeleton of disconnected channel pixels, and connecting them to define the continuous channel network (Passalacqua et al. 2010; Sangireddy et al. 2016). Many of these techniques use static thresholds that are applied to topographic attributes. Clubb et al. (2014) developed a hybrid approach that uses a threshold tangential curvature to distinguish hillslopes from valleys, but then employs chi-plots to automate the delineation of channels from the thresholded terrain. Hooshyar et al. (2016) also used curvature (profile and contour) to define valleys and ridges, but then used unsupervised *k*-means clustering to distinguish the boundaries between channelized and unchannelized sections of the valley zones. A variable flow accumulation approach developed by Heine et al. (2004) uses logistic regression models to predict channel locations.

To evaluate the performance of various high-resolution channel extraction techniques, several studies have used field-surveys of channel heads with

definable banks and sorted bed loads that are typically only found within the perennial and well-defined intermittent portion of the network (Montgomery and Dietrich 1989; Passalacqua et al. 2010; Orlandini et al. 2011; Julian et al. 2012; Elmore et al. 2013; Clubb et al. 2014; Hooshyar et al. 2016), but few have included the poorly defined ephemeral portion of the network (Hastings and Kampf 2014; Jensen et al. 2017). Recently, a growing number of studies have attempted to model streamflow permanence to better understand the extent and duration of wetted channel expansion and contraction and the connectivity between perennially and intermittently flowing streams (Jensen et al. 2018; Ward et al. 2018; Jaeger et al. 2019; Prancevic and Kirchner 2019).

This study explores topographically derived drainage network delineation techniques relative to a comprehensive field survey of ephemeral and perennial channels in two watersheds in Clarksburg, Maryland (Figure 1). An approach to extract the wet-weather (i.e. ephemeral) network from high-

resolution (1.8 m) lidar-derived DEMs was developed using varying levels of topographic openness (TO; Yokoyama et al. 2002) to identify depressions in the landscape and topographic wetness to filter pixels with a greater likelihood of being within the stream network. TO is an angular measure of the degree of dominance or enclosure of a topographic feature relative to its surroundings (Yokoyama et al. 2002). Using a line of sight approach constrained by neighboring elevations within a specified radial search distance, mean angles are measured relative to the zenith (ϕ , positive TO) and nadir (ψ , negative TO) in eight azimuth directions from a central pixel of interest (Figure 2a). Negative TO has been used successfully to extract surface drainage networks in alpine (Sofia et al. 2011) and Martian (Molloy and Stepinski 2007) landscapes, and was used as the primary topographic attribute to identify channel pixels in this study. Topographic wetness index (TWI) was developed within the runoff model TOPMODEL (Beven and Kirkby 1979) and is used to assess the

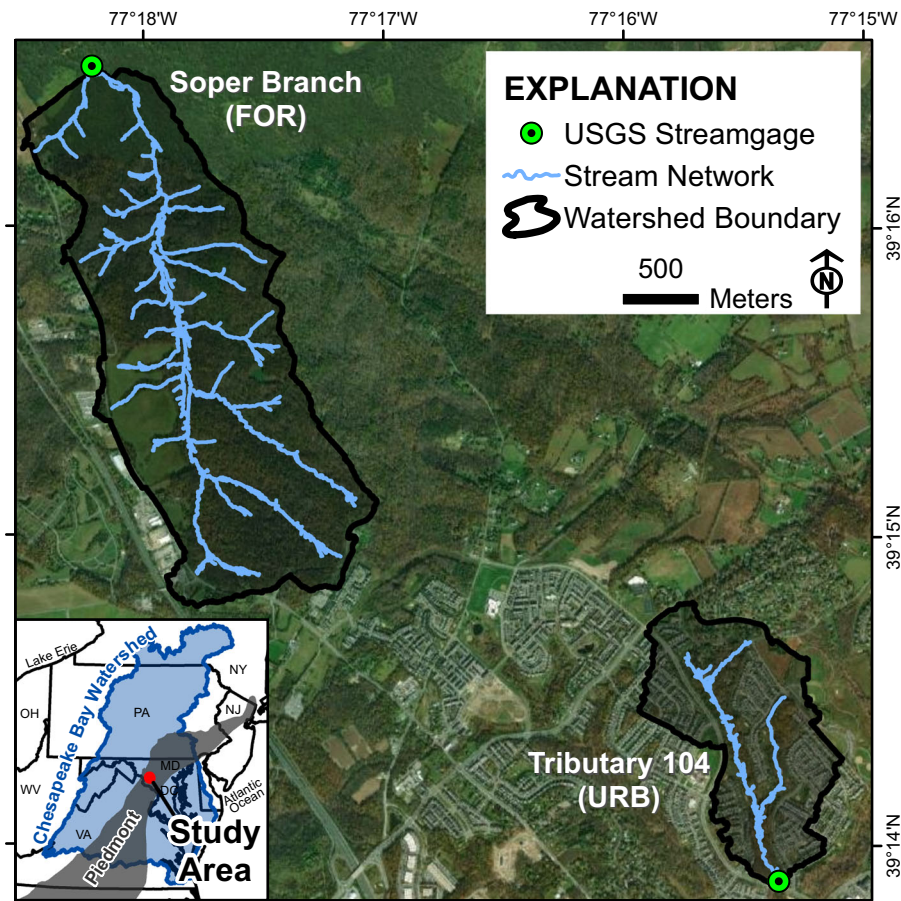


FIGURE 1. Study watersheds in the Maryland Piedmont region. Soper Branch (FOR) is predominantly forested and Tributary 104 (URB) is predominantly urban. Watershed boundaries were delineated from the lidar-derived digital elevation models used in this study (see [DEM Processing](#) section). USGS, United States Geological Survey

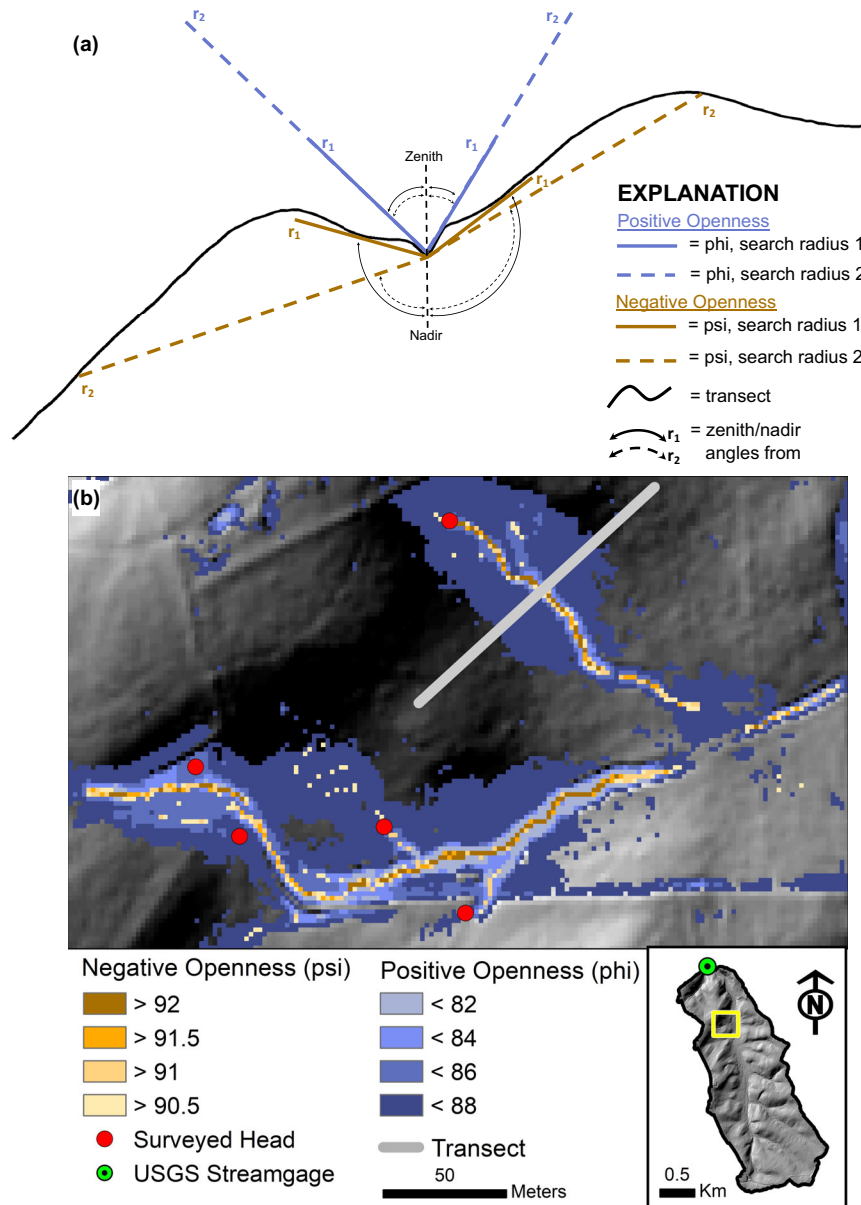


FIGURE 2. (a) Topographic openness calculation for a pixel within a representative transect, and influence of inflection points in the topography based on selected length of search radius, and (b) extent of positive and negative openness thresholds with the locations of field-surveyed channel heads and the representative transect in panel a.

extent of soil saturation and runoff generation potential (Ågren et al. 2014).

Omission, commission, and distances between surveyed and predicted channel heads were examined to assess the ability to accurately represent channel initiation points and overall network structure. This work highlights challenges of mapping ephemeral channel features with high-resolution elevation data, especially in human-modified terrain, and raises important considerations for channel definitions relative to functional and management contexts.

METHODS

Study Sites

For this study, two watersheds in Montgomery County, Maryland, within the Piedmont Physiographic Province were examined (Figure 1). These watersheds have undergone extensive study to evaluate the impacts of development and the effectiveness of stormwater best management practices at the watershed scale (Hogan et al. 2014; Jones et al. 2014; Loperfido et al. 2014; Bhaskar et al. 2016; Hopkins

et al. 2017; Sparkman et al. 2017; Hopkins et al. 2020; Hopkins et al. 2022). Both watersheds are within the Mt. Airy Uplands District, characterized by siltstones and quartzite underlain by crystalline bedrock consisting of phyllite/slate, with average annual precipitation of 106 cm (Reger and Cleaves 2008). The forested watershed, Soper Branch (hereafter referred to as FOR), drains an area of 3.3 km² (see [DEM Processing](#) section) at USGS streamgage 01643395, and the land cover is predominantly classified as deciduous forest (82%) with 4% impervious surface cover (Williams et al. 2018). The urban watershed, Tributary 104 (hereafter referred to as URB), drains an area of 1.1 km² (see [DEM Processing](#) section) at USGS streamgage 01644371 and is a historically agricultural watershed that underwent extensive urban development from 2003 to 2010, with an associated decline in vegetated cover from 97% to 67% and an increase to 31% impervious surface cover (Williams et al. 2018). Although stormwater infrastructure in URB likely plays a key role in dictating watershed hydrology, the purpose of this study was to investigate drainage network structure based on topography alone.

Field Survey of Channel Heads

Channel heads were surveyed in the field between February and April 2013 using a Trimble GeoExplorerXH 6000 handheld unit, providing decimeter positional accuracy after base station correction (Trimble Navigation Limited 2012; Metes et al. 2021). For each watershed, surveys began by walking the mainstem channel upstream from the USGS streamgage (Figure 1), following all major and minor tributaries encountered to all visible points of channel initiation. Initiation points were defined as the most upslope location with evidence of flow-oriented debris and/or vegetation and exposed soil. This definition allowed for the capture of ephemeral channel heads that typically only flow during storm events. All surveys were conducted within two days of the last rainfall to assure ephemeral flow paths were evident. The channel head locations were captured at each channel initiation point along with a brief description of the channel head form (e.g. incised, groundwater seep, knickpoint, and no clear head), presence of flowing water, and a note about the length of the downstream channel. For channels in the urban watershed that terminated at engineered features (e.g. pipe outfalls and detention basins), the surveyed location was taken at the intersection of the channel and engineered feature.

DEM Processing

Airborne lidar was collected on December 28, 2013 (Montgomery County, MD Department of Parks and Planning 2013), and the processed bare earth point cloud covering the study area was acquired from the State of Maryland GIS Data Portal (imap.maryland.gov). A high-resolution DEM (~0.9 m) was interpolated from bare earth lidar points in LAS file format with the commonly used natural neighbor interpolation algorithm (Sibson 1981) in ArcGIS 10.3 (Esri 2011). The DEM was then aggregated to 1.8 m to reduce small-scale surface roughness in the topography. Due to the small watershed size and importance of accuracy, the DEM was manually hydrologically corrected to breach detention basins, culverts, and other barriers to surface flow (Metes et al. 2021). Paths were carved from low points within pits to the next downslope pixel of equal or lesser elevation outside of the pit following detention basin outlets identified from aerial and ground surveys. No attempt was made to account for flow paths within drainage basins or subsurface drainage infrastructure. Straight-line pathways were enforced for all unknown detention basin outlets. The hydrologically corrected DEMs were then filled to resolve any remaining pits and used to generate D8 flow direction and flow accumulation grids (O'Callaghan and Mark 1984; Jenson and Domingue 1988; Esri 2011; Jones et al. 2014). Watershed boundaries for FOR and URB were delineated upstream from each USGS streamgage using the D8 flow direction grid. Both original and hydrologically corrected DEMs were used for stream network delineation.

Delineation of the Field-Surveyed Network

To compare metrics across the entire stream network in FOR and URB watersheds, a field-surveyed drainage network was created from the surveyed channel heads (hereafter referred to as the 'field network'). The surveyed heads in FOR and URB were converted from a point file into a binary raster (1 = head, null = non-head) and used as an accumulation weight along with the D8 flow direction grid to generate a flow accumulation grid where values greater than 0 began at each surveyed channel head. Pixels with a flow accumulation value greater than 0 represented the linear field network. The field network was then post-processed to exclude small offshoot channels that were zero or one pixel long (0–1.8 m) in length, which was equal to or less than the horizontal resolution of the lidar-derived DEM.

Some surveyed channel heads were described in the field notes as ‘questionable’ or ‘potential channels’ and were excluded from analysis (see Metes et al. 2021).

Upslope contributing drainage area was calculated for each post-processed surveyed channel head to compare the range of drainage area necessary for channel initiation in the forested and urban watersheds. To ensure that all upslope drainage area was captured, channel heads in the field network were shifted to the nearest high flow accumulation pixel to account for small offsets in horizontal position between the surveyed and DEM-predicted flow paths arising from DEM and GPS-unit error (see Metes et al. 2021). Heads were initially shifted in ArcGIS 10.3 using Snap Pour Point (ESRI 2011) with a 1.8 m (one pixel) search distance, followed by a manual inspection to adjust heads if they did not snap to the correct high flow accumulation pixel. The shifted channel heads were used as the pour point, along with the D8 flow direction grid, to generate a watershed and calculate drainage area upstream from each surveyed channel head. Contributing drainage areas to each field measured channel head were compared across watersheds using the two-sided Wilcoxon signed-rank tests, implemented in R (Zar 2010; R Core Team 2016). The shifted surveyed channel heads were only used to calculate upstream contributing drainage area. The original surveyed locations of the channel heads were used to calculate distances between surveyed and predicted heads, and to generate the field-surveyed network.

Delineation of the Predicted Networks Derived from Topographic Attributes

A combination of topographic metrics derived from the lidar-derived DEM were used to filter pixels into either channel or non-channel binary grids based on thresholds. A series of topographic thresholds for classifying pixels into the binary grids were evaluated and compared to the field survey. The channel network delineation techniques in this study were calibrated to FOR, which served as the training dataset, and applied to URB as the test dataset to investigate how the altered topography, heterogeneous overland flow paths, and potentially disrupted slope-area processes relating to channel initiation may impact delineation performance (Hastings and Kampf 2014; Jones et al. 2014).

Topographic Wetness Index. TWI was calculated in the raster calculator of ArcMap version 10.3 using the following equation:

$$TWI = \ln(a/\tan\beta), \quad (1)$$

where TWI was calculated as the ratio of the natural log of specific catchment area (a) to the tangent of slope (β). Higher TWI values tend to represent areas that are more saturated; however, specific TWI values change depending on DEM resolution as slope and upslope contributing drainage area will vary with DEM resolution (Wolock and McCabe 2000). A single threshold was applied to filter out lower TWI values that are less likely to include channels. To objectively identify a TWI threshold, a quantile-quantile (Q-Q) plot approach was used to identify the point at which the distribution deviated from normality. This approach has been used with topographic attributes where the deviation from normality is interpreted as the hillslope-valley transition (Lashermes et al. 2007; Passalacqua et al. 2010; Sofia et al. 2011; Clubb et al. 2017). The Q-Q plot of TWI values for FOR was generated and the value at which the upper tail of the distribution deviated from a straight line was selected as the threshold (Figure S1). This same threshold identified in FOR (TWI threshold = 9.6) was also used as the threshold in URB since the modified landscape in the urban watershed may disrupt the distribution of TWI values. TWI was used as an initial filter to constrain the additional topographic attributes used to identify channels.

Topographic Openness. Positive and negative TO were calculated in Python 2.7 (Peters 2015) on the original DEM. The scale of topographic variation detected by TO is dependent on the length of the radial distance parameter (Doneus 2013) (Figure 2a). A longer search radius may reduce the number of smaller depressions that could be considered noise at the expense of missing small poorly defined channel heads that may only show up in a shorter search radius. A search radius of 36 m reduced instances on both ends of the spectrum and was guided by the average valley widths of tributaries in the FOR watershed.

Phi values less than 90 and psi values greater than 90 represent depressions, while values equal to 90 in both measures represent flat areas (Figure 2a). Both components of TO were applied because phi and psi are constrained by different topographic inflection points and tend to highlight different depression-like features (i.e. channel vs. valley bottom) (Figure 2b). Less enclosed or defined features are represented by values close to 90 in both negative and positive TO, and these values are considered “less restrictive” thresholds. As psi values increase in negative TO and phi values decrease in positive TO, only more enclosed or defined depressions are represented, and

these values are considered “more restrictive” thresholds. A range of thresholds that detect both flatter and deeper landscape depressions (psi values >90 for negative and phi values <90 for positive TO) were initially explored to generate a series of stream networks in the FOR watershed, ranging from less to more restrictive. Q-Q plots were also explored for negative and positive TO thresholds in FOR (Figure S2). Only the positive and negative TO pixels overlapping with each other and the previously defined TWI filter were used to define the extent of the predicted stream networks. These final pixels identified as channels were applied as a weight to a D8 flow accumulation to create a contiguous stream network (Figure 3).

The end nodes of each predicted network were used to compare predicted heads with field-surveyed heads. Each predicted head was checked for a corresponding surveyed head to assess the performance of each openness network. An unweighted flow accumulation raster was used to ensure predicted and surveyed heads were only matched if they were on the same flow path. The number of head matches (true positives, TP) and errors of omission (false negative, FN) and commission (false positive, FP) were counted for each predicted network. The omission and commission errors were used to calculate reliability and

sensitivity indices for each network (Orlandini et al. 2011; Clubb et al. 2014). The reliability index (r) is a ratio of TP to the sum of TP and FP (Equation 2) and is a measure of the ability to not produce commission errors:

$$r = \frac{\sum TP}{(\sum TP + \sum FP)} \quad (2)$$

The sensitivity index (s) is a ratio of TP to the sum of TP and FN (Equation 3) and is a measure of the ability to not produce omission errors. A value of 1 is the optimal result for both indices:

$$s = \frac{\sum TP}{(\sum TP + \sum FN)} \quad (3)$$

To further refine appropriate TO thresholds, a rank test was conducted to identify the threshold combinations best representative of the field-surveyed network. Sensitivity and reliability were ranked from 1 to 0. The ratio of the predicted network to field network length was subtracted from 1 and the absolute value was ranked from 0 to 1. The ranks of all three were averaged for a final ranking weighting each metric equally (Table S1). The top three TO threshold combinations resulting from the weighted rank analysis, the least and most restrictive TO threshold combinations, and the TO thresholds resulting from the

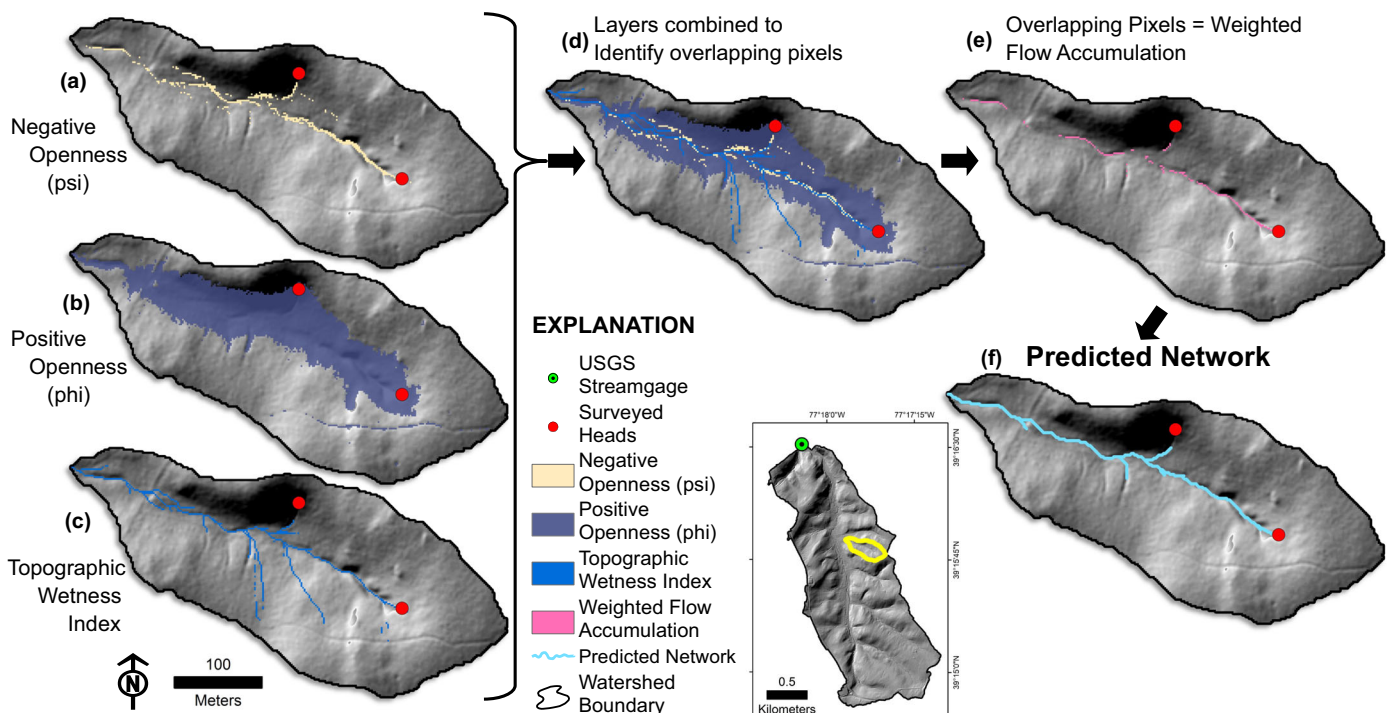


FIGURE 3. Depiction of how topographic filters are combined to arrive at the final drainage network prediction in FOR. Topographic filters (a–c) were combined (d, e) and then an accumulation function was used to connect locations where all three filters overlap. The final predicted network (f) is a representation of where all three filters combined predict a channel.

Q-Q plot analysis were then applied to the URB watershed to generate stream networks.

Delineation of the Accumulation Network. The stream networks created from combinations of TWI and TO were compared to a conventional stream delineation approach using an upslope contributing drainage area threshold applied to the flow accumulation grid to define channel initiation locations (O'Callaghan and Mark 1984), hereafter referred to as the accumulation network. The threshold for each watershed was chosen using the constant drop law, which states that the mean elevation drop across channels within a given Strahler order should not be significantly different from the mean drop in the next higher order (Broscoe 1959; Tarboton et al. 1991; Tarboton and Ames 2001). The TauDEM toolbox (Tarboton 2009) was used to automatically apply the constant drop law in 100-pixel (324 m²) increments to select the minimum contributing drainage area to satisfy the constant drop law. The contributing drainage area thresholds selected for FOR and URB were 9,072 and 12,312 m², respectively.

National Hydrography Dataset. The NHDPlus HR (USGS 2018) was also compared to field-surveyed networks and each predicted network within FOR and URB.

Comparing Predicted and Field-Surveyed Ephemeral Networks

A suite of drainage network metrics was calculated for the field and predicted networks, including Shreve (1966) magnitude, Strahler (1957) stream order, and drainage density. The metrics previously generated for the weighted ranking analysis (ratio of predicted stream length to field network stream length, omission/sensitivity, and commission/reliability) were also calculated for the NHDPlus HR and accumulation networks and included in the stream network comparisons.

Euclidean distances between the predicted and field-surveyed channel heads were calculated and assigned either a positive value if the predicted head was upslope of the surveyed head (over-predicted) or a negative value if the predicted head was downslope of the surveyed head (under-predicted). From the number of upslope (over-predicted) and downslope (under-predicted) heads, Wilcoxon signed-rank tests were used to determine if each network significantly under- or over-predicted the location of heads. Absolute distances between surveyed and predicted heads

were evaluated using the root mean square error (RMSE) (the following equation):

$$RMSE = \sqrt{\sum \frac{(\text{Euclidean distance})^2}{N}}. \quad (4)$$

RESULTS

Field-Surveyed Channel Heads and Network

A total of 245 channel heads were surveyed in FOR, and 81 were surveyed in URB. In post-processing, 77 channel heads were removed because they were small offshoot channels that were zero or one pixel in length, and 7 were removed for being questionable or potential channels (Metes et al. 2021). There were 185 channel heads deemed appropriate for analysis in FOR and 57 channel heads deemed appropriate in URB. The order, length, and drainage densities of the field-surveyed FOR and URB networks are shown in Table 1.

Contributing drainage areas for each surveyed channel head were highly variable in both watersheds. Wilcoxon signed-rank test results revealed a significant difference in contributing drainage areas between the two watersheds ($p < 0.001$), with FOR and URB having median channel head contributing areas of 804 and 217 m², respectively. The distribution varied between the two watersheds with an interquartile range of 2,424 m² in FOR compared to 488 m² in URB (Figure S3).

TO Thresholds Selected for Predicted Stream Networks

A series of negative and positive TO thresholds were explored, ranging from less restrictive values detecting slight depressions in the landscape to more restrictive values identifying more defined depressions (Figure 4; see also Figure 2b). The least restrictive negative TO value ($\psi > 90.5$) captured most pixels containing a surveyed channel head in FOR while also including many non-channel pixels. The least restrictive positive TO value ($\phi < 88$) captured all valleys containing a surveyed channel head in FOR. The most restrictive negative TO threshold ($\psi > 92$) and the most restrictive positive TO threshold ($\phi < 82$) included the majority of pixels falling within known stream channels leading to a surveyed channel head in FOR (Figure 2b).

TABLE 1. Stream network metrics for each openness network, accumulation networks, National Hydrography Dataset plus high resolution (NHDPlus HR), and field-surveyed networks. Metrics include the total number of true positives (TP), omission (false negatives, FN), sensitivity (s), commission (false positives, FP), reliability (r), and root mean square error (RMSE). Metrics that are not calculated for the field-surveyed network are denoted with NA.

Watershed	Network	Number of channel heads (Shreve magnitude)	Strahler order	Network length (km)	Length/field-surveyed network		Drainage density (per km)	TP	FN	s	FP	r	Rank	Number under predicted heads	Number over predicted heads	RMSE of distance between surveyed and predicted heads (m)
					Network length (km)	field-surveyed network length										
FOR	Field-surveyed	185	4	22.6	NA	NA	6.85	NA	NA	NA	NA	NA	NA	NA	NA	NA
FOR	psi 92/phi 82	133	4	16.2	0.72	0.72	4.85	49	136	0.26	84	0.37	8	46 ²	3	63.2
FOR	psi 92/phi 88	206	5	20.8	0.92	0.92	6.23	63	122	0.34	143	0.31	4	49 ²	14	70.0
FOR	psi 91.5/phi 84	253	5	20.9	0.92	0.92	6.26	72	113	0.39	181	0.28	1	58 ²	14	75.1
FOR	psi 91.4/phi 88 ¹	381	5	27.8	1.23	1.23	8.32	89	96	0.48	292	0.23	6	56	33	80.5
FOR	psi 91/phi 84	368	5	24.5	1.08	1.08	7.34	91	94	0.49	277	0.25	2	68 ²	23	71.2
FOR	psi 90.5/phi 82	209	5	19.7	0.87	0.87	5.90	69	116	0.37	140	0.33	4	61 ²	8	86.6
FOR	psi 90.5/phi 88	1,464	6	60.9	2.69	2.69	18.2	128	57	0.69	1,336	0.09	9	45	83 ³	92.9
FOR	Accumulation	56	4	18.8	0.83	0.83	5.70	50	135	0.27	6	0.89	5	35	15	104
FOR	NHDPlus HR	2	2	4.73	0.21	0.21	1.43	2	183	0.011	0	1.0	8	1	1	N/A
URB	Field-Surveyed	57	3	4.82	NA	NA	4.38	NA	NA	NA	NA	NA	NA	NA	NA	NA
URB	psi 92/phi 82	60	4	6.71	1.39	1.39	6.10	12	45	0.21	48	0.20	3	5	7	81.1
URB	psi 92/phi 88	95	4	8.68	1.80	1.80	7.89	20	37	0.35	75	0.21	3	7	13	75.5
URB	psi 91.5/phi 84	131	5	9.78	2.03	2.03	8.89	22	35	0.39	109	0.17	5	8	14	86.3
URB	psi 91.4/phi 88 ¹	189	5	12.8	2.66	2.66	11.6	30	27	0.53	159	0.16	6	15	15	96.7
URB	psi 91/phi 84	189	5	12.1	2.51	2.51	11.0	23	34	0.40	166	0.12	7	10	13	91.8
URB	psi 90.5/phi 82	154	5	10	2.07	2.07	9.09	18	39	0.32	136	0.12	9	10	8	99.9
URB	psi 90.5/phi 88	646	6	28.1	5.83	5.83	25.6	41	16	0.72	605	0.06	8	19	22	99.1
URB	Accumulation	37	5	7.87	1.63	1.63	7.15	8	49	0.14	29	0.22	3	2	6 ³	176
URB	NHDPlus HR	1	1	1.54	0.32	0.32	1.40	1	56	0.018	0	1.0	4	0	1	NA

¹Quantile-quantile (Q-Q) threshold.

²Heads were significantly under-predicted.

³Heads were significantly over-predicted.

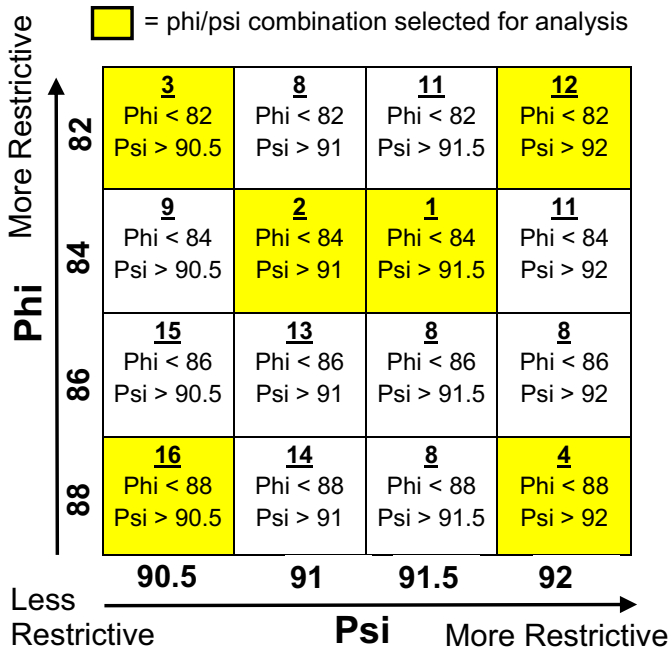


FIGURE 4. Psi/phi threshold combination selected for analysis along with the rank results for FOR (underlined values). The highlighted (yellow) boxes represent the psi/phi threshold combinations used to compare predicted networks against the field-surveyed network. The numbers at the top of each box represent the relative rank, excluding the Q-Q threshold network, of the weighted rank analysis.

The two highest ranked networks most closely resembling the field-surveyed network (based on length and omission/commission error) in FOR had middle levels of restrictiveness for both negative and positive TO (Figure 4). The third ranked network contained a combination of the least restrictive negative TO and the most restrictive positive TO thresholds. Conversely, the fourth ranked network contained the most restrictive negative TO and least restrictive positive TO thresholds. The most restrictive combination of both TO thresholds ranked 12 out of 16 and the least restrictive combination of both TO thresholds ranked last. The Q-Q plot method for selecting TO thresholds resulted in a negative TO value of 91.4 (Figure S2a) and positive TO value of 88 (Figure S2b).

Predicted Stream Network Results

Predicted networks (openness and accumulation) were compared against the field-surveyed network and the NHDPlus HR. The same method to rank the initial phi/psi combinations (Figure 4) was applied to the final openness networks, along with the inclusion of the accumulation network and the NHDPlus HR

for both URB and FOR (Table 1). The rankings of each network were not consistent between FOR and URB. While psi 91.5/phi 84 ranked first in FOR, the same method ranked fifth in URB. The second ranking method in FOR (psi 91/phi 84) ranked eighth out of nine in URB and the eighth ranking method in FOR (psi 92/phi 82) ranked third in URB (tied for third with the psi 92/phi 88 and accumulation networks). The network that ranked similarly in both FOR and URB was psi 90.5/phi 88, performing poorly in both watersheds. The TO threshold combination selected based on Q-Q plots (psi 91.4/phi 88) ranked sixth in both FOR and URB.

The number of TP predicted channels increased as restrictiveness in both TO filters decreased, with the tradeoff of increasing commission errors. The number of TPs was lowest in the accumulation network and NHDPlus HR in URB. In FOR, the NHDPlus HR, accumulation, and most restrictive TO networks had the lowest number of TPs. The omission error was high in all methods, and the networks with the lowest omission errors also had the highest commission errors. Although the NHDPlus HR had no commission error in both watersheds, high omission errors and low length to true length ratios illustrate the large extent to which the NHDPlus HR underrepresents headwater stream networks (Table 1).

Some metrics showed similarities between the FOR and URB networks while other metrics diverged (Table 1). Sensitivity, a measure of omission error, was similar in both watersheds. Reliability, a measure of commission error, was consistently smaller in all the URB networks, indicating a larger fraction of the total predicted heads were commission errors. The length of channels that were commission errors also differed between watersheds. URB consistently exhibited higher length to field length ratios than FOR, reflecting channel extensions along urban conduits in URB (e.g. roads, swales; Figure 5). Elevated drainage densities in URB for both accumulation and openness networks also highlight this result (Table 1). In FOR, many of the FP predicted channels were small first order channels and had little influence on the overall network length, as reflected by length to field length ratios close to one for all openness networks aside from the most restrictive (Table 1).

Distances between Surveyed and Predicted Channel Heads

Euclidean distances were measured between field-surveyed channel heads and corresponding TPs for each predicted network. TPs were classified as an over-prediction if the predicted head was upslope of

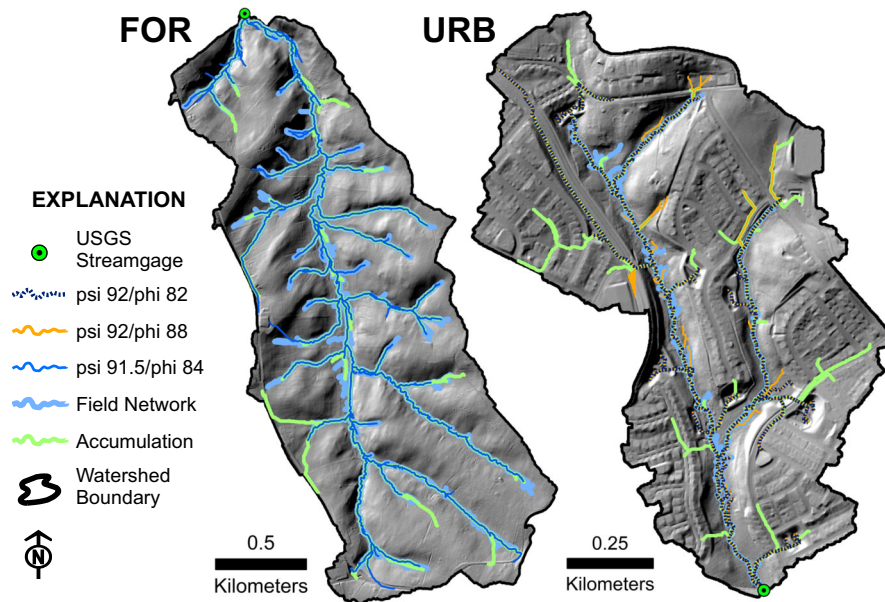


FIGURE 5. Results of the field network (light blue), the accumulation network (green), and top ranked topographic openness network(s) (solid dark blue, orange, or dashed dark blue) in each watershed. In FOR, psi 91.5/phi 84 ranked first (solid dark blue) and in URB psi 92/phi 82 (dashed dark blue) and psi 92/phi 88 (orange) tied with the accumulation network as the highest ranked.

the corresponding surveyed head or an under-prediction if it was downslope from the surveyed head. Boxplots summarizing the signed distances (upslope or downslope) between predicted heads and matched survey heads are displayed in Figure 6. Wilcoxon signed-rank tests indicated the majority of TO networks in FOR significantly under-predicted the head location ($p < 0.001$) with the exception of the least restrictive TO network, which significantly over-predicted the head locations ($p < 0.001$) (Table 1). The only network to neither under- nor over-predict the location of channel heads was the Q-Q technique (psi 91.4/phi 88), with an interquartile range of signed distances near zero (Figure 6). In URB, the only method with a significant result was an over-prediction by the accumulation network ($p < 0.001$, Table 1), with all other methods exhibiting insignificant over-prediction tendencies (Figure 6).

The RMSE of absolute distances between surveyed channel heads and TPs ranged from 63–104 m in FOR and 81–176 m in URB (Table 1). Distances were consistently higher in URB, but only differed by up to 20 m between URB and FOR for each TO network. The two TO networks with the most restrictive phi value (92) accounted for the lowest RMSE and the two TO networks with the least restrictive phi value (90.5) accounted for the largest RMSE among the TO networks in both watersheds. The accumulation network accounted for the largest overall RMSE in both watersheds (Table 1).

DISCUSSION

TO Threshold Variation

Varying the phi and psi thresholds while the TWI threshold remained constant demonstrated how each TO filter contributed to the overall channel network structure. In FOR, the TO threshold combinations that most closely resembled the field network fell in the mid-range for both psi and phi values (Figure 4, rank 1 and 2). The TO combinations with the most and least restrictive threshold combinations (psi 90.5/phi 82 and psi 92/phi 88) also ranked higher than other combinations. This indicates that the TO filter is dominating the resulting network and both negative and positive TO combinations are important contributors to this stream delineation technique. However, in URB, the negative TO threshold exhibited stronger control on the overall network. The two networks containing the most restrictive negative TO threshold (psi >92) most closely resembled the field-surveyed network, despite one network containing the most restrictive positive TO threshold (phi <82) and the other network containing the least restrictive positive TO threshold (phi <88) (Table 1). These two networks both had the lowest Shreve magnitude and network length, but still over-predicted the field-surveyed network, highlighting the difficulty in distinguishing swales and road networks from natural channels using topographic indices (Figure 5).

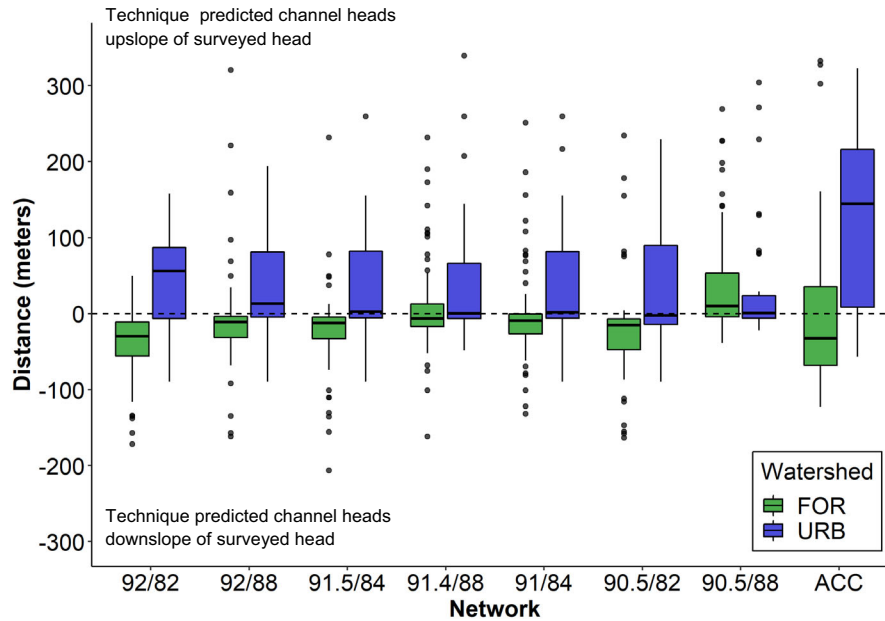


FIGURE 6. Boxplots showing the distances between surveyed channel heads and TPs for each predicted network. Results are only shown for predicted channel heads that had a corresponding matching surveyed channel head (i.e. FPs are excluded). The sample size in each method can be found under TP in Table 1. Boxplot box bounds the 25% and 75% quantiles, solid line shows the median, and points indicate outliers.

To test the utility of including TWI, TO networks were also generated without the TWI filter. In the top ranked network in FOR (psi 91.5/phi 84), omission error dropped slightly from 113 to 105, but commission error increased significantly from 181 to 498. In the least restrictive network in URB (psi 92/phi 82), omission error dropped from 45 to 42 while commission increased from 48 to 163. Although networks generated without TWI have slight improvements in matched heads, the inclusion of this filter greatly improves overall commission errors. Inclusion of additional topographic metrics may also lead to further improvements in the accuracy of predicted networks, but this was outside the scope of this study, which primarily aimed to assess the degree to which TO could be used to detect ephemeral channels.

A balance of commission and omission errors may not always be desirable depending on the intended use of the predicted network (e.g. identifying convergent topography vs. potential habitat), but awareness of the interplay between TO filters and its implications provide a toolset capable of generating varied representations of the drainage structure of a watershed. Exploring multiple levels of threshold restrictiveness and thus generating drainage networks with varying degrees of drainage density also relate to seasonal fluctuations in the wetted extent of the drainage network, which can have useful implications for modeling material flows and runoff upslope from established channels through the watershed. For instance, Blyth and Rodda (1973) monitored the

wetted channel length within a watershed in a humid climate with seasonal variation for one year and found that the length of first order channels varied the most, followed by second and third order channels. Little change in wetted length occurred in fourth order channels. The most restrictive method (psi 92/phi 82) in this study generated third and fourth order channels in FOR and URB with no commission errors while the number of predicted first order channels increased with decreasing restrictiveness (Table 1). The stability observed in higher orders across predicted networks and the substantial variation exhibited by lower orders is consistent with observed patterns of seasonal variation (Blyth and Rodda 1973; Stanley et al. 1997).

Further, intermittent and ephemeral channels comprise the majority of first order channels in humid regions and play an important role in nutrient and sediment transport, biodiversity, land-water interactions, and ecosystem services (Larned et al. 2010; Nikolaidis et al. 2013; Acuña et al. 2014; Hill et al. 2014; USEPA 2015; González-Ferreras and Barquín 2017). Modeling variable drainage network densities more accurately reflects ecological conditions and the effects of climatic variation and change (Stanley et al. 1997), and may highlight hydrologically sensitive portions of the watershed with a more variable source area of runoff generation (Hewlett and Hibbert 1967). This dynamic nature of channels is missing from many topographically based delineation techniques (Prancevic and Kirchner 2019) and widely used network

datasets (NHDPlus HR), thereby misrepresenting the true extent of drainage networks. A large range of contributing drainage areas measured upstream from the field-surveyed networks in both this study and that of Sofia et al. (2011) illustrate why alternative topographically based approaches to simply using drainage area-based thresholds are necessary to capture these processes more accurately in a variety of landscape settings.

Challenges of Detecting Ephemeral Channel Heads

Across predicted networks, 31% of surveyed heads in FOR (57/185) and 28% of surveyed heads in URB (16/57) were never captured (yellow circles, Figure 7). In both URB and FOR, all the heads captured with the accumulation network were also captured with at least one of the TO networks. The average length of missed channels was 20 m in FOR and 11 m in URB. Although shorter and less defined surveyed channels were pruned, some remaining channels may still be below the detection limit of a 1.8-m DEM. Only 5 of the 57 missed channels in FOR and 4 of the 16 missed channels in URB were initially excluded from the TWI filter, so the remaining missed channels were not topographically distinct enough to be identified with TO. Eight of the missed channel heads in FOR and seven in URB were described in the field as marshy or groundwater seepage heads (Metes et al. 2021). Most were captured with TWI alone but also lacked the topographic definition required for capture by TO (Figures 7b and 7d).

The challenge of representing subsurface processes of channel formation with topographic data alone is consistent with Hastings and Kampf (2014) and Orlandini et al. (2011) and further illustrates the limitations of the types of channels that can be mapped with airborne lidar-derived DEMs. However, there are improvements over the more conventional method of using a fixed flow accumulation for identifying the more established channels. Although the most restrictive TO network (psi 92/phi 82) had the highest omission error, it also had the lowest RMSE distance between surveyed and predicted heads (Table 1). The channels that were matched with this method were primarily described in the field as defined channels having clear or incised heads (Metes et al. 2021). The omission error was also comparable to the accumulation network, but the accumulation network also had the largest RMSE distance. While the number of omitted channels were similar, the difference in RMSE between the accumulation and most restrictive TO network illustrates the improved precision of locating more defined channel heads by topographic detection.

Previous studies have primarily conducted channel head surveys in forested or less modified watersheds (Orlandini et al. 2011; Julian et al. 2012; Clubb et al. 2014; Hastings and Kampf 2014). In this study, comprehensive surveys were conducted in both forested and urban watersheds to capture the diversity of channel head forms present. The field survey in this study was expanded from the classic channel head definition of concentrated flow within steepened banks to include all ephemeral channels, and

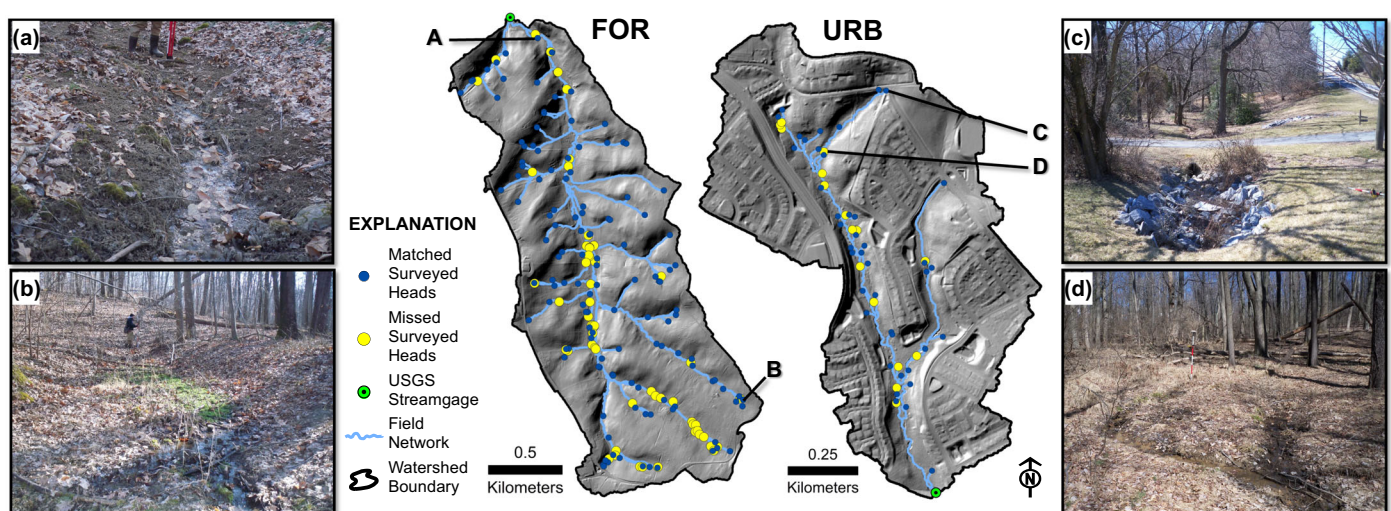


FIGURE 7. Surveyed channel heads matched in at least one of the predicted networks (dark blue) and surveyed heads missed in all networks (yellow). Field-derived networks are shown in light blue. Most channel heads missed by all methods were small offshoots or poorly defined channels (b, d) rather than major tributaries. Head a shows a poorly defined channel that was matched in at least one method and head c shows a matched head in the urban network originating just upstream of a culvert. Photographs by Daniel Jones, USGS.

discrepancies between the openness networks described here and others in the literature could be due to differences in channel head definitions. For example, Orlandini et al. (2011) and Clubb et al. (2014) documented high sensitivity values when comparing their delineation methods against traditional channel head survey data, suggesting more false positives than false negatives. While a direct performance comparison for capturing traditional channel heads was out of the scope of this study, the extension into the ephemeral portion of the network resulted in omission error increases and a low sensitivity. Ephemeral channels are not fixed features, and this study demonstrates the challenges with identifying the location of these features using fixed topographic thresholds.

Management Implications

Identifying potential areas of runoff generation, such as the swales, roads, and extension of channels upslope from stormwater ponds in URB (Figure 5) may provide a topographically based proxy for the increased hydrologic efficiency commonly attributed to impervious surfaces in urban systems (Corbett et al. 1997; Jankowsky et al. 2013; Jones et al. 2014; Prancevic and Kirchner 2019). This information can be applied to help managers identify locations where sediment, nutrients, and other contaminants may concentrate and enter streams during precipitation events (Gellis et al. 2020). Including human constructed features in the predicted networks would potentially provide a more efficient and highly dissected network than more commonly used network representations (e.g. NHDPlus HR). Similarly, the variable network extents offered by the TO methods may provide a representation of seasonal variations in network extents for unmodified catchments. Therefore, accurate representations of the more dynamic ephemeral portions of a watershed are important for designing effective management and conservation plans (González-Ferreras and Barquín 2017; Skoulikidis et al. 2017).

Considerations for Future Method Applications

Underlying limitations with topographic data, such as DEM quality, vertical and horizontal accuracy, and horizontal resolution, are important considerations for applications in other watersheds. Topographic indices are sensitive to DEM processing and DEM horizontal resolution due to controls exerted by small-scale topography rather than hillslope position in higher-resolution DEMs (e.g. less than 5 m resolution). For example, Walker et al. (2021) found various

flow direction algorithms and hydrologic correction methods had an influence on estimating drainage area upstream from gullies. Thomas et al. (2017) found 0.25-m horizontal resolution DEMs tended to over-predict runoff risk, and a horizontal resolution of 1–2 m is more optimal for modeling hydrologically sensitive areas in agricultural watersheds. The 1.8-m DEMs used in the study presented here were on the coarser side of this 1–2 m range, and they were derived from quality level (QL) three lidar according to the USGS 3D Elevation Program guidelines (Heidemann 2018). Most newly acquired lidar is QL two or better (Heidemann 2018), so it may be worthwhile to investigate how the techniques explored herein behave with DEMs of differing horizontal resolution and quality. DEMs finer than 1.8 m horizontal resolution may capture the small, less defined channels that were largely underrepresented across TO networks, but may cause higher commission errors (Orlandini et al. 2011). Since the methods introduced here use TWI, which is derived from a D8 flow direction grid, other flow direction algorithms may influence the resulting TWI filter.

Land use could also be considered when selecting an optimal channel delineation method (Passalacqua et al. 2012). The best TO thresholds in FOR were not the same as URB, and even the most restrictive TO thresholds resulted in an over-prediction of the stream network in URB. The geomorphic characteristics of false channels in URB networks are difficult to distinguish from natural stream channels, so reliance on direct feature detection-based methods will capture them as well (Sangireddy et al. 2016). The same criteria for identifying channel heads in FOR were applied to URB. For channels that terminated at engineered features (e.g. pipe outfalls, detention basins), heads were surveyed at the intersection of the channel and engineered feature. Many of the commission errors in URB were along swales and roads that behave like ephemeral channels; therefore, it would be valuable to consider a survey that includes stormwater infrastructure to assess commission errors more accurately. If excluding urban infrastructure from the drainage network is a desired outcome, additional filters may need to be introduced, such as buffering areas within a certain proximity to impervious surfaces. However, additional runoff and channel initiation factors such as climate, geology, soil properties, land use, and both natural and human-modified variations in topography may exhibit varying controls across different settings (Montgomery 1999; Julian et al. 2012; Bezerra et al. 2020), so additional landscape metrics or filters introduced to the methodology may not have universal application. Testing this variability across multiple regions was outside the scope of this study. The parameters

used to delineate the highest ranked networks in URB and FOR may be applicable to other headwater watersheds in the Maryland Piedmont with similar land use, but further analysis is required to assess how each predicted network delineated from these TO thresholds would perform in other regions.

Various TO thresholds were explored, and the performance differed between watersheds. In the future, it may be desirable to automate the selection of ϕ and ψ to produce the optimal network structure. However, optimal structure may vary with intended use (e.g. climate projections, management scenarios, habitat selection) and could be the subject of intensive study in and of itself. Furthermore, methods tested in forested or relatively undisturbed watersheds are often assumed to be applicable to urban watersheds. As illustrated in this study, the same methods generate different results between urban and forested watersheds, highlighting the need for better methods to delineate urban drainage networks.

CONCLUSIONS

The purpose of this study was to explore the utility of two topographic attributes, TWI and TO, to extract the wet-weather portion of channel networks in both a forested and urban environment. Extracted networks were compared against comprehensive field surveys of ephemeral and perennial channel heads in each watershed, and against two commonly used drainage network representations (the NHDPlus HR and a flow accumulation threshold) to evaluate performance. Many ephemeral channels lacked strong topographic signatures and were thus missed in all the delineation methods evaluated, highlighting challenges of remotely mapping the ephemeral portion of a stream network with high-resolution lidar-derived DEMs. The topographic attributes used to map the channel network did not detect small ephemeral channels without the inclusion of false channels. But the location of these ‘false’ channels can be informative to watershed managers to highlight likely runoff patterns. There were clear improvements in predicted stream networks delineated using the TO method introduced in this study compared with more simplistic NHDPlus HR or flow accumulation methods, especially for delineating drainage networks that better represent true drainage density and ephemeral channel locations. The method introduced here highlights the utility of TO for detecting stream channels.

Results also highlight the challenges of applying methods developed in less modified landscapes to urban systems with altered surface hydrology.

Differences between the urban and forested watershed highlight the importance of considering the function of stormwater features, their connection to the wet-weather portion of a stream network, and how various definitions and delineation techniques of the network change the appearance of hydrologic connectivity within an urban watershed.

DATA AVAILABILITY STATEMENT

The channel head survey data and lidar-derived DEMs used in this study are available at <https://doi.org/10.5066/P9OVTCK4>.

SUPPORTING INFORMATION

Additional supporting information may be found online under the Supporting Information tab for this article: A table with the data used for the weighted rank, figures showing the Q-Q plots for TWI, ϕ , and ψ , and boxplots showing the contributing drainage area for each surveyed channel head.

ACKNOWLEDGMENTS

The authors thank Lillian Gorman Sanisaca (USGS) for R coding assistance, and three anonymous reviewers for their suggestions and edits. This work was funded by the United States Geological Survey Core Science System Mission Area as part of the Land Change Science Program. Any use of trade, firm, or product names is for descriptive purposes only and does not imply endorsement by the United States Government.

AUTHOR CONTRIBUTIONS

Marina J. Metes: Conceptualization; data curation; formal analysis; methodology; visualization; writing – original draft; writing – review and editing. Daniel K. Jones: Conceptualization; data curation; formal analysis; funding acquisition; investigation; methodology; writing – original draft; writing – review and editing. Matthew E. Baker: Conceptualization; methodology; writing – review and editing. Andrew J. Miller: Conceptualization; methodology; writing – review and editing. Dianna M. Hogan: Conceptualization; funding acquisition; writing – review and editing. J.V. Loperfido: Conceptualization; investigation; writing – review and editing. Kristina G. Hopkins: Conceptualization; funding acquisition; project administration; writing – review and editing.

LITERATURE CITED

- Acuña, V., T. Datry, J. Marshall, D. Barceló, C.N. Dahm, A. Ginebreda, G. McGregor, S. Sabater, K. Tockner, and M.A. Palmer. 2014. "Why Should we Care about Temporary Waterways?" *Science* 343 (6175): 1080–81. <https://doi.org/10.1126/science.1246666>.
- Ågren, A.M., W. Lidberg, M. Strömberg, J. Ogilvie, and P.A. Arp. 2014. "Evaluating Digital Terrain Indices for Soil Wetness Mapping — A Swedish Case Study." *Hydrology & Earth System Sciences* 18 (9): 3623–34. <https://doi.org/10.5194/hess-18-3623-2014>.
- Baker, M.E., D.E. Weller, and T.E. Jordan. 2007. "Effects of Stream Map Resolution on Measures of Riparian Buffer Distribution and Nutrient Retention Potential." *Landscape Ecology* 22 (7): 973–92. <https://doi.org/10.1007/s10980-007-9080-z>.
- Band, L.E. 1993. "Extraction of Channel Networks and Topographic Parameters from Digital Elevation Data." In *Channel Network Hydrology*, edited by K.J. Beven and M.J. Kirkby, 13–42. Hoboken, NJ: John Wiley.
- Beven, K.J., and M.J. Kirkby. 1979. "A Physically Based Variable Contributing Area Model of Catchment Hydrology." *Hydrological Sciences Bulletin* 24 (1): 43–69. <https://doi.org/10.1080/02626667909491834>.
- Bezerra, M.O., M. Baker, M.A. Palmer, and S. Filoso. 2020. "Gully Formation in Headwater Catchments under Sugarcane Agriculture in Brazil." *Journal of Environmental Management* 270: 110271. <https://doi.org/10.1016/j.jenvman.2020.110271>.
- Bhaskar, A.S., D.M. Hogan, and S.A. Archfield. 2016. "Urban Base Flow with Low Impact Development." *Hydrological Processes* 30 (18): 3156–71. <https://doi.org/10.1002/hyp.10808>.
- Blyth, K., and J.C. Rodda. 1973. "A Stream Length Study." *Water Resources Research* 9 (5): 1454–61. <https://doi.org/10.1029/WR009i005p01454>.
- Brooks, R.T., and E.A. Colburn. 2011. "Extent and Channel Morphology of Unmapped Headwater Stream Segments of the Quabbin Watershed, Massachusetts." *Journal of the American Water Resources Association* 47 (1): 158–68. <https://doi.org/10.1111/j.1752-1688.2010.00499.x>.
- Broscoe, A.J. 1959. "Quantitative Analysis of Longitudinal Stream Profiles of Small Watersheds." Office of Naval Research, Project NR 389–042. Technical Report No. 18. New York, NY: Columbia University Department of Geology.
- Clubb, F.J., S.M. Mudd, D.T. Milodowski, M.D. Hurst, and L.J. Slater. 2014. "Objective Extraction of Channel Heads from High-Resolution Topographic Data." *Water Resources Research* 50 (5): 4283–304. <https://doi.org/10.1002/2013WR015167>.
- Clubb, F.J., S.M. Mudd, D.T. Milodowski, D.A. Valters, L.J. Slater, M.D. Hurst, and A.B. Limaye. 2017. "Geomorphometric Delineation of Floodplains and Terraces from Objectively Defined Topographic Thresholds." *Earth Surface Dynamics* 5 (3): 369–85. <https://doi.org/10.5194/esurf-5-369-2017>.
- Colson, T., J. Gregory, J. Dorney, and P. Russell. 2008. "Topographic and Soil Maps Do Not Accurately Depict Headwater Stream Networks." *National Wetlands Newsletter* 30 (3): 25–28.
- Colson, T.P., J.D. Gregory, H. Mitasova, and S.A.C. Nelson. 2006. "Comparison of Stream Extraction Models Using Lidar DEMs." In *American Water Resources Association — Spring Conference*, Houston, TX.
- Corbett, C.W., M. Wahl, D.E. Porter, D. Edwards, and C. Moise. 1997. "Nonpoint Source Runoff Modeling a Comparison of a Forested Watershed and an Urban Watershed on the South Carolina Coast." *Journal of Experimental Marine Biology and Ecology* 213 (1): 133–49. [https://doi.org/10.1016/S0022-0981\(97\)00013-0](https://doi.org/10.1016/S0022-0981(97)00013-0).
- Doneus, M. 2013. "Openness as Visualization Technique for Interpretative Mapping of Airborne Lidar Derived Digital Terrain Models." *Remote Sensing* 5 (12): 6427–42. <https://doi.org/10.3390/rs5126427>.
- Downing, J.A., J.J. Cole, C.M. Duarte, J.J. Middelburg, J.M. Melack, Y.T. Prairie, P. Kortelainen, R.G. Striegl, W.H. McDowell, and L.J. Tranvik. 2012. "Global Abundance and Size Distribution of Streams and Rivers." *Inland Waters* 2 (4): 229–36. <https://doi.org/10.5268/IW-2.4.502>.
- Elmore, A.J., J.P. Julian, S.M. Guinn, and M.C. Fitzpatrick. 2013. "Potential Stream Density in Mid-Atlantic U.S. Watersheds." *PLoS One* 8 (8): e74819. <https://doi.org/10.1371/journal.pone.0074819>.
- Elmore, A.J., and S.S. Kaushal. 2008. "Disappearing Headwaters: Patterns of Stream Burial Due to Urbanization." *Frontiers in Ecology and the Environment* 6 (6): 308–12. <https://doi.org/10.1890/070101>.
- ESRI. 2011. *ArcGIS Desktop (Release 10)*. Redlands, CA: Environmental Systems Research Institute. <https://www.esri.com/>.
- Gellis, A.C., C.C. Fuller, P.C. Van Metre, B.J. Mahler, C. Welty, A.J. Miller, L.A. Nibert, Z.J. Clifton, J.J. Malen, and J.T. Kemper. 2020. "Pavement Alters Delivery of Sediment and Fallout Radionuclides to Urban Streams." *Journal of Hydrology* 588: 124855. <https://doi.org/10.1016/j.jhydrol.2020.124855>.
- Gomi, T., R.C. Sidle, and J.S. Richardson. 2002. "Understanding Processes and Downstream Linkages of Headwater Systems: Headwaters Differ from Downstream Reaches by their Close Coupling to Hillslope Processes, more Temporal and Spatial Variation, and their Need for Different Means of Protection from Land Use." *Bioscience* 52 (10): 905–16. [https://doi.org/10.1641/0006-3568\(2002\)052\[0905:UPADLO\]2.0.CO;2](https://doi.org/10.1641/0006-3568(2002)052[0905:UPADLO]2.0.CO;2).
- González-Ferreras, A.M., and J. Barquín. 2017. "Mapping the Temporary and Perennial Character of Whole River Networks." *Water Resources Research* 53: 6709–24. <https://doi.org/10.1002/2017WR020390>.
- Hansen, W.F. 2001. "Identifying Stream Types and Management Implications." *Forest Ecology and Management* 143 (1): 39–46. [https://doi.org/10.1016/S0378-1127\(00\)00503-X](https://doi.org/10.1016/S0378-1127(00)00503-X).
- Hastings, B.E., and S.K. Kampf. 2014. "Evaluation of Digital Channel Network Derivation Methods in a Glaciated Subalpine Catchment." *Earth Surface Processes and Landforms* 39 (13): 1790–802. <https://doi.org/10.1002/esp.3566>.
- Heidemann, H.K. 2018. "Lidar Base Specification (Ver. 1.3, February 2018)." U.S. Geological Survey Techniques and Methods, Book 11, Chap. B4, 101. <https://doi.org/10.3133/tm11B4>.
- Heine, R.A., C.L. Lant, and R.R. Sengupta. 2004. "Development and Comparison of Approaches for Automated Mapping of Stream Channel Networks." *Annals of the Association of American Geographers* 94 (3): 477–90. <https://doi.org/10.1111/j.1467-8306.2004.00409.x>.
- Hewlett, J.D., and A.R. Hibbert. 1967. "Factors Affecting the Response of Small Watersheds to Precipitation in Humid Areas." *Forest Hydrology* 1: 275–90. 10.1177/2F0309133309338118.
- Hill, B.H., R.K. Kolka, F.H. McCormick, and M.A. Starry. 2014. "A Synoptic Survey of Ecosystem Services from Headwater Catchments in the United States." *Ecosystem Services* 7: 106–15. <https://doi.org/10.1016/j.ecoser.2013.12.004>.
- Hill, R.A., M.H. Weber, S.G. Leibowitz, A.R. Olsen, and D.J. Thornbrugh. 2016. "The Stream-Catchment (StreamCat) Dataset: A Database of Watershed Metrics for the Conterminous United States." *Journal of the American Water Resources Association* 52 (1): 120–28. <https://doi.org/10.1111/1752-1688.12372>.
- Hogan, D.M., S.T. Jarnagin, J.V. Loperfido, and K. Van Ness. 2014. "Mitigating the Effects of Landscape Development on Streams in Urbanizing Watersheds." *Journal of the American Water Resources Association* 50 (1): 163–78. <https://doi.org/10.1111/jawr.12123>.

- Hooshyar, M., D. Wang, S. Kim, S.C. Medeiros, and S.C. Hagen. 2016. "Valley and Channel Networks Extraction Based on Local Topographic Curvature and k-Means Clustering of Contours." *Water Resources Research* 52: 8081–102. <https://doi.org/10.1002/2015WR018479>.
- Hopkins, K.G., A.S. Bhaskar, S.A. Woznicki, and R.M. Fanelli. 2020. "Changes in Event-Based Streamflow Magnitude and Timing after Suburban Development with Infiltration-Based Stormwater Management." *Hydrological Processes* 34 (2): 387–403. <https://doi.org/10.1002/hyp.13593>.
- Hopkins, K.G., J.V. Loperfido, L.S. Craig, G.B. Noe, and D.M. Hogan. 2017. "Comparison of Sediment and Nutrient Export and Runoff Characteristics from Watersheds with Centralized Versus Distributed Stormwater Management." *Journal of Environmental Management* 203: 286–98. <https://doi.org/10.1016/j.jenvman.2017.07.067>.
- Hopkins, K.G., S.A. Woznicki, B.M. Williams, C.C. Stillwell, E. Naibert, M.J. Metes, D.K. Jones, et al. 2022. "Lessons Learned from 20 y of Monitoring Suburban Development with Distributed Stormwater Management in Clarksburg, Maryland, USA." *Freshwater Science* 41 (3). <https://doi.org/10.1086/719360>.
- Istanbulluoglu, E., D.G. Tarboton, R.T. Pack, and C. Luce. 2002. "A Probabilistic Approach for Channel Initiation." *Water Resources Research* 38 (12): 1325–39. <https://doi.org/10.1029/2001WR000782>.
- Jaeger, K.L., R. Sando, R.R. McShane, J.B. Dunham, D.P. Hockman-Wert, K.E. Kaiser, K. Hafen, J.C. Risley, and K.W. Blasch. 2019. "Probability of Streamflow Permanence Model (PROSPER): A Spatially Continuous Model of Annual Streamflow Permanence throughout the Pacific Northwest." *Journal of Hydrology X* 2: 100005. <https://doi.org/10.1016/j.hydroa.2018.100005>.
- James, L.A., and K.J. Hunt. 2010. "The LiDAR-Side of Headwater Streams: Mapping Channel Networks with High-Resolution Topographic Data." *Southeastern Geographer* 50 (4): 523–39. <https://doi.org/10.1353/sgo.2010.0009>.
- James, L.A., D.G. Watson, and W.F. Hansen. 2007. "Using LiDAR Data to Map Gullies and Headwater Streams under Forest Canopy: South Carolina, USA." *Catena* 71 (1): 132–44. <https://doi.org/10.1016/j.catena.2006.10.010>.
- Jankowfsky, S., F. Branger, I. Braud, J. Gironás, and F. Rodriguez. 2013. "Comparison of Catchment and Network Delineation Approaches in Complex Suburban Environments: Application to the Chaudanne Catchment, France." *Hydrological Processes* 27 (25): 3747–61. <https://doi.org/10.1002/hyp.9506>.
- Jensen, C.K., K.J. McGuire, and P.S. Prince. 2017. "Headwater Stream Length Dynamics across Four Physiographic Provinces of the Appalachian Highlands." *Hydrological Processes* 31 (19): 3350–63. <https://doi.org/10.1002/hyp.11259>.
- Jensen, C.K., K.J. McGuire, Y. Shao, and C. Andrew Dolloff. 2018. "Modeling Wet Headwater Stream Networks across Multiple Flow Conditions in the Appalachian Highlands." *Earth Surface Processes and Landforms* 43 (13): 2762–78. <https://doi.org/10.1002/esp.4431>.
- Jenson, S.K., and J.O. Domingue. 1988. "Extracting Topographic Structure from Digital Elevation Data for Geographic Information System Analysis." *Photogrammetric Engineering and Remote Sensing* 54 (11): 1593–600. <https://pubs.er.usgs.gov/publication/70142175>.
- Jones, D.K., M.E. Baker, A.J. Miller, S.T. Jarnagin, and D.M. Hogan. 2014. "Tracking Geomorphic Signatures of Watershed Suburbanization with Multitemporal LiDAR." *Geomorphology* 219: 42–52. <https://doi.org/10.1016/j.geomorph.2014.04.038>.
- Julian, J.P., A.J. Elmore, and S.M. Guinn. 2012. "Channel Head Locations in Forested Watersheds across the Mid-Atlantic United States: A Physiographic Analysis." *Geomorphology* 177–178: 194–203. <https://doi.org/10.1016/j.geomorph.2012.07.029>.
- Larned, S.T., T. Datry, D.B. Arscott, and K. Tockner. 2010. "Emerging Concepts in Temporary-River Ecology." *Freshwater Biology* 55 (4): 717–38. <https://doi.org/10.1111/j.1365-2427.2009.02322.x>.
- Lashermes, B., E. Foufoula-Georgiou, and W.E. Dietrich. 2007. "Channel Network Extraction from High Resolution Topography Using Wavelets." *Geophysical Research Letters* 34 (23). <https://doi.org/10.1029/2007GL031140>.
- Lindsay, J.B. 2006. "Sensitivity of Channel Mapping Techniques to Uncertainty in Digital Elevation Data." *International Journal of Geographical Information Science* 20 (6): 669–92. <https://doi.org/10.1080/13658810600661433>.
- Loperfido, J.V., G.B. Noe, S.T. Jarnagin, and D.M. Hogan. 2014. "Effects of Distributed and Centralized Stormwater Best Management Practices and Land Cover on Urban Stream Hydrology at the Catchment Scale." *Journal of Hydrology* 519: 2584–95. <https://doi.org/10.1016/j.jhydrol.2014.07.007>.
- McNamara, J.P., A.D. Ziegler, S.H. Wood, and J.B. Vogler. 2006. "Channel Head Locations with Respect to Geomorphologic Thresholds Derived from a Digital Elevation Model: A Case Study in Northern Thailand." *Forest Ecology and Management* 224 (1–2): 147–56. <https://doi.org/10.1016/j.foreco.2005.12.014>.
- Messenger, M.L., B. Lehner, C. Cockburn, N. Lamouroux, H. Pella, T. Snelder, K. Tockner, T. Trautmann, C. Watt, and T. Datry. 2021. "Global Prevalence of Non-perennial Rivers and Streams." *Nature* 594 (7863): 391–97. <https://doi.org/10.1038/s41586-021-03565-5>.
- Metes, M.J., D.K. Jones, and J.V. Loperfido. 2021. "Ephemeral Channel Heads and Digital Elevation Models Used to Extract Stream Networks in Clarksburg, MD (Ver 2.0, October 2021)." U.S. Geological Survey Data Release. <https://doi.org/10.5066/P9OVTCK4>.
- Meyer, J.L., D.L. Strayer, J.B. Wallace, S.L. Eggert, G.S. Helfman, and N.E. Leonard. 2007. "The Contribution of Headwater Streams to Biodiversity in River Networks." *Journal of the American Water Resources Association* 43 (1): 86–103. <https://www.fs.usda.gov/treesearch/pubs/31625>.
- Meyer, J.L., and J.B. Wallace. 2001. "Lost Linkages and Lotic Ecology: Rediscovering Small Streams." In *Ecology: Achievement and Challenge*, edited by M.C. Press, N.J. Huntly, and S. Levin, 295–317. London, UK: Blackwell Science.
- Molloy, I., and T.F. Stepinski. 2007. "Automatic Mapping of Valley Networks on Mars." *Computers & Geosciences* 33 (6): 728–38. <https://doi.org/10.1016/j.cageo.2006.09.009>.
- Montgomery County, MD Department of Parks and Planning. 2013. "Montgomery County, MD Aerial Lidar Terrain Data 2014." Bel Air, MD. https://lidar.geodata.md.gov/metadata/Montgomery/2013/Montgomery_Lidar_dem_2014.xml.
- Montgomery, D.R. 1999. "Process Domains and the River Continuum." *Journal of the American Water Resources Association* 35 (2): 397–410. <https://doi.org/10.1111/j.1752-1688.1999.tb03598.x>.
- Montgomery, D.R., and W.E. Dietrich. 1988. "Where Do Channels Begin?" *Nature* 336: 232–34. <https://doi.org/10.1038/336232a0>.
- Montgomery, D.R., and W.E. Dietrich. 1989. "Source Areas, Drainage Density, and Channel Initiation." *Water Resources Research* 25 (8): 1907–18. <https://doi.org/10.1029/WR025i008p01907>.
- Montgomery, D.R., and W.E. Dietrich. 1992. "Channel Initiation and the Problem of Landscape Scale." *Science* 255 (5046): 826–30. <https://doi.org/10.1126/science.255.5046.826>.
- Montgomery, D.R., and E. Foufoula-Georgiou. 1993. "Channel Network Source Representation Using Digital Elevation Models." *Water Resources Research* 29 (12): 3925–34. <https://doi.org/10.1029/93WR02463>.
- Nikolaidis, N.P., L. Demetropoulou, J. Froebrich, C. Jacobs, F. Gallart, N. Prat, A. Lo Porto, et al. 2013. "Towards Sustainable Management of Mediterranean River Basins: Policy

- Recommendations on Management Aspects of Temporary Streams." *Water Policy* 15 (5): 830–49. <https://doi.org/10.2166/wp.2013.158>.
- O'Callaghan, J.F., and D.M. Mark. 1984. "The Extraction of Drainage Networks from Digital Elevation Data." *Computer Vision, Graphics, and Image Processing* 28 (3): 323–44. [https://doi.org/10.1016/S0734-189X\(84\)80011-0](https://doi.org/10.1016/S0734-189X(84)80011-0).
- Orlandini, S., P. Tarolli, G. Moretti, and G. Dalla Fontana. 2011. "On the Prediction of Channel Heads in a Complex Alpine Terrain Using Gridded Elevation Data." *Water Resources Research* 47 (2). <https://doi.org/10.1029/2010WR009648>.
- Passalacqua, P., P. Belmont, and E. Foufoula-Georgiou. 2012. "Automatic Geomorphic Feature Extraction from Lidar in Flat and Engineered Landscapes." *Water Resources Research* 48 (3). <https://doi.org/10.1029/2011WR010958>.
- Passalacqua, P., T. Do Trung, E. Foufoula-Georgiou, G. Sapiro, and W.E. Dietrich. 2010. "A Geometric Framework for Channel Network Extraction from Lidar: Nonlinear Diffusion and Geodesic Paths." *Journal of Geophysical Research: Earth Surface* 115 (F1). <https://doi.org/10.1029/2009JF001254>.
- Peters, M. 2015. "Variable Terrestrial GPS Telemetry Detection Rates: Part 7 — Openness Python Script Version 2.0." U.S. Geological Survey Software Release. <https://doi.org/10.5066/F7PG1PT2>.
- Prancevic, J.P., and J.W. Kirchner. 2019. "Topographic Controls on the Extension and Retraction of Flowing Streams." *Geophysical Research Letters* 46 (4): 2084–92. <https://doi.org/10.1029/2018GL081799>.
- R Core Team. 2016. *R: A Language and Environment for Statistical Computing*. Vienna, Austria: R Foundation for Statistical Computing. <https://www.R-project.org/>.
- Reger, J.P., and E.T. Cleaves. 2008. *Draft Physiographic Map of Maryland and Explanatory Text for the Physiographic Map of Maryland* (Open File Report 08–03-01). Baltimore, MD: Maryland Geological Survey. https://training.fws.gov/courses/csp/csp3200/resources/documents/map_of_maryland_description.pdf.
- Roy, A.H., A.L. Dybas, K.M. Fritz, and H.R. Lubbers. 2009. "Urbanization Affects the Extent and Hydrologic Permanence of Headwater Streams in a Midwestern U.S Metropolitan Area." *Journal of the North American Benthological Society* 28 (4): 911–28. <https://doi.org/10.1899/08-178.1>.
- Sangireddy, H., C.P. Stark, A. Kladzyk, and P. Passalacqua. 2016. "GeoNet: An Open Source Software for the Automatic and Objective Extraction of Channel Heads, Channel Network, and Channel Morphology from High Resolution Topography Data." *Environmental Modelling & Software* 83: 58–73. <https://doi.org/10.1016/j.envsoft.2016.04.026>.
- Shanafield, M., S.A. Bourke, M.A. Zimmer, and K.H. Costigan. 2021. "An Overview of the Hydrology of Non-perennial Rivers and Streams." *Wiley Interdisciplinary Reviews: Water* 8 (2): 1504. <https://doi.org/10.1002/wat2.1504>.
- Shreve, R.L. 1966. "Statistical Law of Stream Numbers." *The Journal of Geology* 74 (1): 17–37. <https://doi.org/10.1086/627137>.
- Sibson, R. 1981. "A Brief Description of Natural Neighbor Interpolation." In *Interpolating Multivariate Data*, edited by V. Barnett, 21–36. New York: John Wiley & Sons.
- Skoulidakis, N.T., S. Sabater, T. Datry, M.M. Morais, A. Buffagni, G. Dörflinger, S. Zogaris, et al. 2017. "Non-perennial Mediterranean Rivers in Europe: Status, Pressures, and Challenges for Research and Management." *Science of the Total Environment* 577: 1–18. <https://doi.org/10.1016/j.scitotenv.2016.10.147>.
- Sofia, G., P. Tarolli, F. Cazorzi, and G. Dalla Fontana. 2011. "An Objective Approach for Feature Extraction: Distribution Analysis and Statistical Descriptors for Scale Choice and Channel Network Identification." *Hydrology and Earth System Sciences* 15: 1387–402. <https://doi.org/10.5194/hess-15-1387-2011>.
- Sparkman, S.A., D.M. Hogan, K.G. Hopkins, and J.V. Loperfido. 2017. "Modeling Watershed-Scale Impacts of Stormwater Management with Traditional Versus Low Impact Development Design." *Journal of the American Water Resources Association* 53 (5): 1081–94. <https://doi.org/10.1111/1752-1688.12559>.
- Stanley, E.H., S.G. Fisher, and N.B. Grimm. 1997. "Ecosystem Expansion and Contraction in Streams." *Bioscience* 47 (7): 427–35. <https://doi.org/10.2307/1313058>.
- Stewart, J.S., G.E. Schwarz, J.W. Brakebill, and S.D. Preston. 2019. "Catchment-Level Estimates of Nitrogen and Phosphorus Agricultural Use from Commercial Fertilizer Sales for the Conterminous United States, 2012." U.S. Geological Survey Scientific Investigations Report 2018–5145. <https://doi.org/10.3133/sir20185145>.
- Strahler, A.N. 1957. "Quantitative Analysis of Watershed Geomorphology." *Transactions of the American Geophysical Union* 38 (6): 913–20. <https://doi.org/10.1029/TR038i006p00913>.
- Tarboton, D.G. 2009. "Terrain Analysis Using Digital Elevation Models (TauDEM) 4.0." <http://hydrology.usu.edu/taudem/taudem4.0/index.html>.
- Tarboton, D.G., and D.P. Ames. 2001. "Advances in the Mapping of Flow Networks from Digital Elevation Data." Paper Presented at World Water and Environmental Resources Congress, Orlando, FL. [https://doi.org/10.1061/40569\(2001\)166](https://doi.org/10.1061/40569(2001)166).
- Tarboton, D.G., R.L. Bras, and I. Rodriguez-Iturbe. 1991. "On the Extraction of Channel Networks from Digital Elevation Data." *Hydrological Processes* 5 (1): 81–100. <https://doi.org/10.1002/hyp.3360050107>.
- The Navigable Waters Protection Rule. 2020. "Definition of 'Waters of the United States', 85 Fed. Reg. § 22250 (Final Rule June 22, 2020) (To Be Codified at 33 C.F.R. Pt. 328 and 40 C.F.R. Pts. 110, 112, 116, 117, 120, 122, 230, 232, 300, 302, and 401)."
- Thomas, I.A., P. Jordan, O. Shine, O. Fenton, P.-E. Mellander, P. Dunlop, and P.N.C. Murphy. 2017. "Defining Optimal DEM Resolutions and Point Densities for Modelling Hydrologically Sensitive Areas in Agricultural Catchments Dominated by Microtopography." *International Journal of Applied Earth Observation and Geoinformation* 54: 38–52. <https://doi.org/10.1016/j.jag.2016.08.012>.
- Thornbrugh, D.J., S.G. Leibowitz, R.A. Hill, M.H. Weber, Z.C. Johnson, A.R. Olsen, J.E. Flotemersch, J.L. Stoddard, and D.V. Peck. 2018. "Mapping Watershed Integrity for the Conterminous United States." *Ecological Indicators* 85: 1133–48. <https://doi.org/10.1016/j.ecolind.2017.10.070>.
- Tribe, A. 1990. "Automated Recognition of Valley Heads from Digital Elevation Models." *Earth Surface Processes and Landforms* 16 (1): 33–49. <https://doi.org/10.1002/esp.3290160105>.
- Tribe, A. 1992. "Automated Recognition of Valley Lines and Drainage Networks from Grid Digital Elevation Models: A Review and a New Method." *Journal of Hydrology* 139 (1–4): 263–93. [https://doi.org/10.1016/0022-1694\(92\)90206-B](https://doi.org/10.1016/0022-1694(92)90206-B).
- Trimble Navigation Limited. 2012. "GeoExplorer® 6000 Series: User Guide." https://sendai.hmdc.harvard.edu/cga_website_files/PDF_misc/GPS/GeoExpl6000_UserGde_ENG.pdf.
- USEPA (U.S. Environmental Protection Agency). 2015. *Connectivity of Streams and Wetlands to Downstream Waters: A Review and Synthesis of the Scientific Evidence*. EPA/600/R-14/475F. Washington, D.C.: Office of Research and Development, U.S. Environmental Protection Agency. <https://cfpub.epa.gov/ncea/risk/recordisplay.cfm?deid=296414>.
- USGS (U.S. Geological Survey). 2018. "USGS National Hydrography Dataset Plus High Resolution (NHDPlus HR) for 4-Digit Hydrologic Unit — 0207 (Published 20180813)." <https://www.sciencebase.gov/catalog/item/5d30c269e4b01d82ce84a929>.
- Vance-Borland, K., K. Burnett, and S. Clarke. 2009. "Influence of Mapping Resolution on Assessments of Stream and Streamside Conditions: Lessons from Coastal Oregon, USA." *Aquatic*

- Conservation: Marine and Freshwater Ecosystems* 19 (3): 252–63. <https://doi.org/10.1002/aqc.967>.
- Viger, R.J., A. Rea, J.D. Simley, and K.M. Hanson. 2016. “NHDPlusHR: A National Geospatial Framework for Surface-Water Information.” *Journal of the American Water Resources Association* 52 (4): 901–05. <https://doi.org/10.1111/1752-1688.12429>.
- Walker, J.P., and G.R. Willgoose. 1999. “On the Effect of Digital Elevation Model Accuracy on Hydrology and Geomorphology.” *Water Resources Research* 35 (7): 2259–68. <https://doi.org/10.1029/1999WR900034>.
- Walker, S.J., A.I. van Dijk, S.N. Wilkinson, and P.B. Hairsine. 2021. “A Comparison of Hillslope Drainage Area Estimation Methods Using High-Resolution DEMs with Implications for Topographic Studies of Gullies.” *Earth Surface Processes and Landforms* 46 (11): 2229–47. <https://doi.org/10.1002/esp.5171>.
- Ward, A.S., N.M. Schmadel, and S.M. Wondzell. 2018. “Simulation of Dynamic Expansion, Contraction, and Connectivity in a Mountain Stream Network.” *Advances in Water Resources* 114: 64–82. <https://doi.org/10.1016/j.advwatres.2018.01.018>.
- Wieczorek, M.E., S.E. Jackson, and G.E. Schwarz. 2018. “Select Attributes for NHDPlus Version 2.1 Reach Catchments and Modified Network Routed Upstream Watersheds for the Conterminous United States.” U.S. Geological Survey Data Release. <https://doi.org/10.5066/F7765D7V>.
- Williams, B.M., H. Tarekegn, D.M. Hogan, S.T. Jarnagin, S.A. Woznicki, and K.G. Hopkins. 2018. “Land Use Land Cover, 1998–2013, Clarksburg (Montgomery County, MD).” U.S. Geological Survey Data Release. <https://doi.org/10.5066/F7TH8KZV>.
- Wolock, D.M., and G.J. McCabe. 2000. “Differences in Topographic Characteristics Computed from 100- and 1000-m Resolution Digital Elevation Model Data.” *Hydrological Processes* 14 (6): 987–1002. [https://doi.org/10.1002/\(SICI\)1099-1085\(20000430\)14:6<987::AID-HYP980>3.0.CO;2-A](https://doi.org/10.1002/(SICI)1099-1085(20000430)14:6<987::AID-HYP980>3.0.CO;2-A).
- Yokoyama, R., M. Shirasawa, and R.J. Pike. 2002. “Visualizing Topography by Openness: A New Application of Image Processing to Digital Elevation Models.” *Photogrammetric Engineering & Remote Sensing* 68 (3): 257–65.
- Zar, J.H. 2010. *Biostatistical Analysis* (Fifth Edition). Upper Saddle River, NJ: Prentice Hall.
- Zhang, W., and D.R. Montgomery. 1994. “Digital Elevation Model Grid Size, Landscape Representation, and Hydrologic Simulations.” *Water Resources Research* 30 (4): 1019–28. <https://doi.org/10.1029/93WR03553>.